Published in final edited form as:
Cancer Res. 2010 April 1; 70(7): 2613–2623. doi:10.1158/0008-5472.CAN-09-3185.

ANTITUMOR ACTIVITY OF HYALURONIC ACID SYNTHESIS INHIBITOR 4-METHYLUMBELLIFERONE IN PROSTATE CANCER CELLS

Vinata B. Lokeshwar[1,2,3], **Luis E. Lopez**[1], **Daniel Munoz**[1], **Andrew Chi**[1], **Samir P. Shirodkar**[1], **Soum D. Lokeshwar**, **Diogo O. Escudero**[2], **Neetika Dhir**[1], and **Norman Altman**[4]

[1]Department of Urology, University of Miami Miller School of Medicine, Miami, Florida, 33101, U.S.A.

[2]Department of Cell Biology and Anatomy, University of Miami Miller School of Medicine, Miami, Florida, 33101, U.S.A.

[3]Department of Sylvester Comprehensive Cancer Center, University of Miami Miller School of Medicine, Miami, Florida, 33101, U.S.A.

[4]Department of Pathology, University of Miami Miller School of Medicine, Miami, Florida, 33101, U.S.A.

Abstract

4-methylumbelliferone (4-MU) is a hyaluronic acid (HA) synthesis inhibitor with anticancer properties; the mechanism of its anticancer effects is unknown. We evaluated the effects of 4-MU on prostate cancer cells. 4-MU inhibited proliferation, motility and invasion of DU145, PC3-ML, LNCaP, C4-2B and/or LAPC-4 cells. At IC_{50} for HA synthesis (0.4 mM), 4-MU induced > 3-fold apoptosis in prostate cancer cells, which could be prevented by HA addition. 4-MU induced caspase-8, -9 and -3 activation, PARP cleavage, up-regulation of Fas-L, Fas, FADD and DR4 and down regulation of bcl-2, phospho-bad, bcl-XL, phospho-Akt, phospho-IKB, phospho-ErbB2 and phospho-EGFR. At IC_{50}, 4-MU also caused > 90% inhibition of NFkB reporter activity which was prevented partially by HA addition. With the exception of caveolin-1, HA prevented the 4-MU induced down regulation of HA receptors (CD44, RHAMM), matrix-degrading enzymes (MMP-2, MMP-9), IL-8, and chemokine receptors (CXCR1, CXCR4, CXCR7) at protein and mRNA levels. Expression of myristoylated-Akt rescued 4-MU induced apoptosis and inhibition of cell growth and IL-8, RHAMM, HAS2, CD44 and MMP-9 expression. Oral administration of 4-MU significantly decreased PC3-ML tumor growth (> 3-fold), when treatment was started either on the day of tumor cell injection or after the tumors became palpable, without organ toxicity, changes in serum chemistry or body weight. Tumors from 4-MU treated animals showed reduced microvessel density (~ 3-fold) and HA expression but increased TUNEL positive cells and expression of apoptosis-related molecules. Therefore, anticancer effects of 4-MU, an orally bioavailable and relatively non-toxic agent, are primarily mediated by inhibition of HA signaling.

Keywords

Hyaluronic acid; Hyaluronic acid receptors; 4-methylumbelliferone; prostate cancer

✦**Address for Correspondence:** Vinata B. Lokeshwar, Ph.D., Professor and Co-Director Division of Urology Research, Department of Urology (M-800), University of Miami Miller School of Medicine, P.O. Box 016960, Miami, Florida 33101, Phone: (305) 243-6321, Fax: (305) 243-6893, vlokeshw@med.miami.edu.

INTRODUCTION

Hyaluronic acid is a non-sulfated glycosaminoglycan made up of D-glucuronic acid and N-acetyl-D-glucosamine. HA expression is elevated in a variety of tumors (1). In prostate tumor tissues, elevated HA levels are contributed by both tumor-associated stroma and tumor cells and together with HYAL-1 hyaluronidase (HAase) predict disease progression (2–6). HA regulates several cellular functions (7–9). In the human genome there are three HA synthase (HAS) genes, HAS1, HAS2 and HAS3, each of the HAS synthesizes HA of different molecular mass (10–12). Silencing HAS genes in tumor cells inhibits cell proliferation, invasion and motility *in vitro* and tumor growth and metastasis *in vivo* (11–17). For example, knockdown of HAS1 expression induces Fas-mediated apoptosis and inhibits invasion *in vitro* and causes inhibition of tumor growth, infiltration and angiogenesis in xenografts (16). In prostate cancer cells, HA-synthase expression requires HYAL-1 hyaluronidase to promote tumor growth, metastasis and angiogenesis (13,14). These results are consistent with our observations that HYAL-1 is a molecular determinant of tumor growth, invasion and angiogenesis (18,19) and suggest that a finely regulated cellular HA-hyaluronidase system promotes tumor growth and progression.

Cellular effects of HA are mediated through HA receptors, CD44 and RHAMM. CD44-HA interaction induces activation of receptor tyrosine kinases (20–22). HAS1 knockdown inhibits ErbB2 activation and transcriptionally down regulates CD44 (16). HA-induced CD44-EGF receptor (EGFR) interaction and EGFR activation promotes cellular motility through Akt signaling and increased expression of MMP-2/MMP-9 (22–25). HA also induces IL-8 and stromal-derived factor-1 (SDF-1) receptor (CXCR4) expression through NFkB activation (25–30). IL-8 expression promotes tumor growth, angiogenesis and androgen independent growth of prostate cancer cells (31). HA-RHAMM interaction also induces intracellular signaling (32). Therefore, inhibition of HA synthesis in tumor cells should help control tumor growth and progression.

4-Methylumbelliferone (4-MU; 7-Hydroxy-4-methylcoumarin) is a HA synthesis inhibitor with choleretic and anti-spasmodic properties (Heparvit™). In mammalian cells, HA is synthesized by HAS, using UDP-glucuronic acid (UGA) and UDP-N-acetyl-D-glucosamine precursors. UGA is synthesized when UGA-transferase transfers UDP to glucuronic acid. In cells treated with 4-MU, UGA-transferase transfers glucuronic acid onto 4-MU. This depletes the intracellular pool of UGA, resulting in inhibition of HA synthesis (33–37). 4-MU also down regulates HAS2 and HAS3 expression (38). Oral administration of 4-MU (600 mg/kg/day) reduces metastases by 64% in the B16 melanoma model (34). Currently, intracellular signaling events involved in the antitumor effects of 4-MU are unknown. In this study we evaluated the antitumor activity of 4-MU in prostate cancer cells and in a xenograft model.

MATERIALS AND METHODS

Cell culture

Prostate cancer cells LNCaP, DU145, PC3-ML were cultured in RPMI 1640 + 10% FBS + gentamicin (18,31). LAPC-4 cells were maintained in Iscove's medium with 7.5 % fetal bovine serum (FBS) and 1 nM dihydrotestosterone (31). C4-2B cells were cultured in T-Medium + 10% FBS + gentamicin.

Reagents

4-MU was purchased from Sigma-Aldrich (St. Louis, MO). Hyaluronic acid sodium salt was purchased from MBL (Woburn, MA) and Lifecore Biomedical (Chaska, MN). All of the antibodies and constructs used in this study are described in the Supplemental Information.

HA ELISA-like assay

Twenty-four hour cultures of PC3-ML and DU145 cells (10^5 cells/well; 12-well plates) were treated with 4-MU, coumerin or 4-hydroxy coumerin (0 – 0.8 mM) for 36 hours. Conditioned media were analyzed by HA ELISA-like assays and HA levels were normalized to cell number (6).

Cell proliferation and apoptosis

Prostate cancer cells (2.0×10^4 cells/well; 24-well plates) cultured in growth medium were exposed to 4-MU (0–0.6 mM) and counted after 72 h. Alternatively, cells (1.5×10^4) were exposed to 4-MU (0.4 mM) and counted every 24 h. For the apoptosis assay, cells plated on 24-well plates were exposed to 4-MU (0–0.6 mM). Following 24 or 48 h incubation, apoptosis was analyzed using the Cell Death ELISA Plus kit (Roche Diagnostics; Pleasanton, CA). The apoptosis index was calculated as $O.D._{450\ nm}$ per 20,000 cells. In some experiments, 50 μg/ml HA was added to the wells at the time of 4-MU addition.

Motility and invasion assays

Matrigel™ invasion assay was carried out as described previously (16,18,19) except that 4-MU was added in both chambers of the Transwell; for details, please see supplemental information. To neutralize the effect of 4-MU on cell growth, percent invasion or motility was calculated as [O.D. bottom chamber ÷ O.D. (top + bottom chambers)] ×100.

Immunoblot analyses and time course

Prostate cancer cells were exposed to 4-MU (0 – 0.6 mM) for 24 – 48 h. For time course experiments, 14 h cultures of PC3-ML were exposed to 4-MU (0.4 mM) for 4, 8, 12, 18 and 24 h. The cell lysates (~20 μg/ml) were analyzed by immunoblotting using specific antibodies. In some wells, 50 μg/ml HA was added at the time of 4-MU addition. The intensity of each protein band, following chemiluminescence, was determined using Kodak image analysis software.

Real time RT-PCR (Q-PCR) assays

PC3-ML cells were treated with 4-MU +/− HA (50 μg/ml) for 24 – 48 h; HA was added at the same time as 4-MU. Q-PCR was performed using the iQ SYBR Green Supermix (BioRad, Hercules, CA) and the primers described in Table 1 (Supplement) (16). The mRNA levels were normalized to β-actin. In some experiments, 4-MU treated cells were exposed to actinomycin D (10-μg/ml) and the rate of mRNA degradation was determined by Q-PCR. Q-PCR was also performed 72 h after transfecting PC3-ML cells with 1) either CD44 siRNA, RHAMM siRNA, 2) both CD44 and RHAMM siRNAs (50 nM each), or 3) control Non-targeting siRNA (Dharmacon, Denver, CO) (40).

Transient transfection

PC3-ML cells were transiently co-transfected with pNF-κB-luc and pGL4.74[*hRluc*/TK] plasmids. Eight hours following transfection, the cells were exposed to 4-MU (0.4 mM) in the presence or absence of 50-μg/ml HA. Following 24 h incubation, the firefly luciferase and Renilla luciferase activities were assayed (39).

PC3-ML cells were also transiently transfected with a myr-Akt plasmid and then treated with 4-MU (0.4 mM). Cell growth, apoptosis, gene expression (Q-PCR) and NFkB reporter assays were conducted after 48 h. For details please see supplemental information.

Tumor xenografts

PC3-ML cell suspension (2×10^6 cells/0.1 ml) was mixed 1:1 with Matrigel™ and implanted subcutaneously in the dorsal flank of 5–6 month old athymic mice. There were ten mice per treatment group. The mice were gavaged twice daily with vehicle (phosphate buffered saline) or 4-MU (225 mg/kg or 450 mg/kg). The treatment began either on the day of injection or on day 7 when the tumors became palpable. Tumor volume was measured twice weekly (16,18). Animals were euthanized when tumor volume in the control animals exceeded 0.5 cc. A portion of each tumor was either flash frozen for preparing tumor extracts or fixed for immunohistochemistry (to localize HA and microvessels or TUNEL positive cells; ref 16,18, 19,31,40). For details on tumor extract preparation, determination of microvessel density (MVD) and the TUNEL assay please see supplemental section. Serum chemistry was performed by the Division of Veterinary Resources, University of Miami. Lung, kidney, liver, seminal vesicles, prostate and testes were fixed and histology was performed by the Division of Veterinary Resources.

RESULTS

4-MU inhibited HA synthesis and cell proliferation in prostate cancer cells

PC3-ML cells secrete ~ 4–5-fold higher HA levels when compared to DU145 cells (6). We therefore measured the effect of 4-MU on HA synthesis in PC3-ML and DU145 cells. As shown in Figure 1 A, 4-MU inhibited HA synthesis in both cell lines (IC_{50} ~ 0.4 mM). In contrast, coumerin or 4-hydroxycoumerin did not inhibit HA synthesis (Figure 1 A).

Effect of 4-MU on cell growth is shown in Figure 1 B. After 72 h treatment, 4-MU inhibited the growth of all five prostate cancer cell lines (IC_{50} 0.2 – 0.4 mM). At $\geq IC_{50}$, the differences in cell numbers between untreated and 4-MU-treated samples were statistically significant ($P < 0.001$; unpaired t-test). Presence of HA during incubation with 4-MU prevented 4-MU induced inhibition of PC3-ML cell growth (IC_{50} ~ 0.8 mM in the presence of HA versus 0.4 mM for 4-MU alone; Figure 1 B). In the presence of 4-MU, cell detachment did not exceed 10% of the total cell count. Time course experiments showed that 4-MU inhibited the growth of prostate cancer cells at each time point (Figure 1 C; $P < 0.001$; unpaired t-test). 4-MU treatment also caused a change in cell morphology. As shown in Figure 1 D, within 48 h of 4-MU treatment, PC3-ML cells became irregular in shape with projections. HA addition (50 μg/ml) partially prevented this change in cell morphology (data not shown).

4-MU induced apoptosis in prostate cancer cells

We next examined whether the growth inhibition by 4-MU was due to induction of apoptosis. 4-MU induced apoptosis in prostate cancer cells, in a dose-dependent manner with ≥ 3-fold induction of apoptosis at IC_{50} (0.4 mM; Figure 2 A). As shown in Figure 2 B, 4-MU caused 2–3 fold induction of apoptosis in PC3-ML cells (mean apoptosis index: untreated, 0.096; 0.2 mM, 0.22; 0.4 mM, 0.3; $P < 0.001$; Bonferroni multiple comparison test). However, addition of HA prevented this effect (mean apoptosis index: 0.2 mM 4-MU + HA, 0.1; 0.4 mM 4-MU + HA, 0.13; $P > 0.05$; Bonferroni multiple comparison test). These results show that the effect of 4-MU on cell growth and apoptosis was due to inhibition of HA synthesis.

As shown in Figure 2 C, in PC3-ML and LAPC-4 cells, 4-MU induced activation of pro-apoptotic effectors, caspase-8, caspase-9 and caspase-3 (2–4 fold) and PARP cleavage. Figure 2 D shows that 4-MU induced up-regulation of Fas-L, Fas, FADD and DR4 and bid cleavage (p15bid); at 0.4 mM concentration there was 1.8–3-fold up-regulation of these death-inducing signaling complex (DISC) proteins. Eight hours following 4-MU treatment there was up-regulation of Fas-L, Fas and DR4, with a maximal increase occurring by 12 h (Figure 2 D). 4-MU also caused a decrease in bcl-2 (> 4-fold), bcl-XL (< 2-fold) and phospho-bad (> 2-fold)

levels. Addition of HA during 4-MU treatment, prevented the up- or down-regulation of each of the signaling molecules in the apoptosis cascade (Figure 2 C and D).These results show that 4-MU decreased cell survival mainly by inducing the extrinsic pathway of apoptosis.

HA is known to induce ErbB2 and Akt activation; Akt activation induces survival by phosphorylating bad at ser136 (16,20–22). 4-MU induced a dose-dependent decrease in phospho-Akt and phospho-ErbB2 levels (Figure 2 D). At 0.4 mM concentration, the decrease was ~ 4-fold for phospho-ErbB2 and > 2-fold for phospho-Akt and HA prevented the 4-MU induced decrease in phospho-Akt and phospho-ErbB2 levels.

4-MU inhibits invasion and chemotactic motility

Since HA promotes tumor cell migration and invasion, we examined whether 4-MU inhibits the invasive potential of prostate cancer cells. As shown in Figure 3 A and B, 4-MU induced a dose-dependent decrease the invasive activity of PC3-ML and DU145 cells. At 0.4 mM concentration, the inhibition was ~ 67% in both cell types ($P < 0.001$; Bonferroni multiple comparison test). However, in the presence of HA, 4-MU caused only 15% –20% inhibition of invasion (Figure 3 A and B; $P > 0.05$).

4-MU also inhibited chemotactic motility of PC3-ML and DU145 cells (Figure 3 C). At 0.4 mM concentration, 4-MU caused a 55% and 43% inhibition of chemotactic motility in PC3-ML and DU145 cells, respectively ($P<0.01$; unpaired t-test). HA of addition reduced this inhibition to 25% and 17%, respectively, for PC3-ML and DU145 cells. Since HA prevented 4-MU induced inhibition of chemotactic motility and invasion, 4-MU, very likely, inhibits these properties by inhibiting HA synthesis.

4-MU down regulates HA-receptor expression and regulators of invasion and motility

CD44-HA interaction induces matrix metalloproteinase expression (23,24) and HAS1 and HAS2 knockdown transcriptionally down regulates CD44 (16,17). We, therefore, examined whether 4-MU down regulates HA-receptors (CD44 and/or RHAMM), HA-synthases and/or MMP-2 and MMP-9 levels. Consistent with our previous findings (41), PC3-ML cells express the 90 kDa standard-form of CD44 (CD44s; Figure 3 D). Furthermore, 4-MU caused a dose-dependent decrease in CD44, RHAMM, HAS2, MMP-2 and MMP-9 levels (2–3-fold decrease at 0.4 mM concentration). Addition of HA at the same time as 4-MU addition, prevented the down regulation of CD44, RHAMM, MMP-2, MMP-9 and HAS2 (Figure 3 D). Since the HAS2 siRNA down regulated the protein band detected by HAS2 antibody, it demonstrated that the anti-HAS2 antibody was specific (Figure 3 D).

In prostate cancer, elevated caveolin-1 expression correlates with disease progression and promotes cell survival and angiogenesis (42). As shown in Figure 3 D, 4-MU induced ~ 10-fold decrease in caveolin-1 expression; however, addition of HA did not prevent this decrease.

4-MU also induced a dose-dependent down regulation of CD44, RHAMM, MMP-2, MMP-9 and caveolin-1 mRNA levels (Figure 4 A and C). The mean CD44s mRNA levels in untreated samples (15.15 ± 0.85) were 9.2-times higher than CD44v mRNA levels (1.65 ± 0.25), confirming that PC3-ML cells mainly express CD44s form. At 0.4 mM concentration, 4-MU decreased CD44s, CD44v, RHAMM, HAS2, MMP-2 and MMP-9 mRNA levels by 2.5–3-fold and caveolin-1 mRNA levels by 7.7-fold ($P < 0.001$ for each mRNA). 4-MU did not alter HAS1 and HAS3 mRNA levels (data not shown). The addition of HA completely prevented the 4-MU-induced decrease in CD44, RHAMM, HAS2, MMP-2 and MMP-9 mRNA levels (Figure 4 B) and caused a partial prevention of the decrease in HAS2 mRNA levels (No 4-MU: 3.7 ± 0.2; 0.4 mM 4-MU: 2.4 ± 0.3). However, HA did not prevent the decrease in caveolin-1 levels

(Figure 4 C). Comparison between the effect of 4-MU and 4-MU + HA treatments on the expression of each gene presented in Figures 4 A – C is shown in Table 2 –supplement.

The decrease in mRNA levels of the genes described above was most likely transcriptional, since the mRNA degradation rates in the presence and absence of 4-MU were similar in PC3-ML cells treated with actinomycin-D (data not shown).

Since HA prevented the effect of 4-MU on gene expression, we determined whether down regulation of CD44 and/or RHAMM expression by siRNA, would similarly affect the gene expression. Down regulation CD44 or RHAMM by themselves did not significantly alter MMP-2, MMP-9 or caveolin-1 mRNA levels (data not shown). However, simultaneous down regulation of CD44 and RHAMM decreased the mRNA levels of both receptors over 95% and of HAS2 and MMP-9 levels by ~ 35–40%; no down regulation of caveolin-1 mRNA was observed (Figure 4 D). The data related to the down regulation of other genes shown in the Figure are discussed below.

Since 4-MU is currently the only known compound with a well characterized biochemical mechanism of inhibition of HA synthesis (35,36), we examined whether down regulation of HAS2, CD44, RHAMM, or both CD44 and RHAMM mimics the biological effects of 4-MU. As shown in Figure S1-A (supplement), down regulation of HAS2, CD44, RHAMM and CD44 + RHAMM caused 68.5%, 47.7%, 57.7% and 64% inhibition of cell growth, respectively; in each case the decrease was statistically significant ($P < 0.001$; unpaired t-test). Down regulation of each of these genes induced 1.5 – 2-fold induction of apoptosis within 48 h (Figure S1-B).

4-MU down regulates IL-8, IL-8 receptors and CXCR4

HA induces EGFR and Akt activation, and up-regulates IL-8 and CXCR4 through NFkB activation (26–30). Therefore, we examined the effect of 4-MU on EGFR and Akt phosphorylation. As shown in Figure 5 A, 4-MU decreased phospho-EGFR and phospho-Akt levels with similar kinetics (~ 50% decrease by 8 h), while the down regulation of CD44 and RHAMM levels by 4-MU occurred at later time points (~ 50% in 12 h).

Akt activates NFkB by phosphorylating IKKα, which in turn, phosphorylates IKB, targeting it for degradation. As shown in Figure 5 A, 4-MU decreased phospho-IKB levels > 4-fold after 12 h treatment, with an increase in total IKB levels at 18 and 24 h. HA addition, prevented 4-MU-induced decrease in phospho-IKB levels. Effect of 4-MU treatment on NFkB-promoter luciferase reporter activity is shown in Figure 5 B. At 0.4 mM, 4-MU inhibited NFkB reporter activity by 83% (51.8 ± 6.8 versus 8.8 ± 2.3; $P < 0.001$ unpaired t-test), and HA partially prevented this inhibition (relative activity: 29.6 ± 2.0). Down regulation of CD44, RHAMM, or both receptors simultaneously, as well as down regulated NFkB reporter activity by 54–70% (Figure 5 B).

We next examined the effect of 4-MU on IL-8 (CXCR1 and CXCR2) and SDF-1 (CXCR4 and CXCR7) receptors. As shown in Figure 5 A, 4-MU caused a dose decrease in CXCR1, CXCR4 and CXCR7 levels (IC_{50}: 0.4 mM), with no alterations in CXCR2 levels. Furthermore, HA addition prevented this decrease (Figure 5 A). Q-PCR analyses showed that 4-MU decreased CXCR1, CXCR4 and CXCR7 mRNA levels by 2–2.7-fold and IL-8 mRNA levels by ~ 10-fold at 0.4 mM concentration (Figure 5 C). 4-MU also caused a dose-dependent decrease in IL-8 levels (~5-fold at 0.4 mM). 4-MU did not alter SDF-1 mRNA levels (data not shown). Addition of HA completely prevented the decrease caused by 4-MU in CXCR1, CXCR4, CXCR7 mRNA levels and a partially prevented the decrease in IL-8 mRNA and IL-8 levels (from 5–10-fold to 2-fold; Figure 5 D). Simultaneous down regulation of both CD44 and RHAMM by siRNA also induced a 35–70% down regulation in CXCR1, IL-8 and CXCR7

levels, but no decrease in CXCR4 levels (Figure 4 D). Therefore, it is likely that 4-MU inhibits IL-8 and chemokine receptor expression by negatively regulating HA-HA-receptor interaction.

Effect of constitutive Akt activation on 4-MU-induced cellular effects

To understand the mechanism by which 4-MU might inhibit cell growth, gene expression and induce apoptosis, we evaluated various effects of 4-MU in PC3-ML cells transfected with a myristoylated-Akt plasmid (m-Akt, constitutively active Akt). As shown in Figure S1-A (supplement), m-Akt transfection increased total Akt levels by 3-fold and p-Akt levels by over 10-fold when compared to the vector control. p-Akt levels were not appreciably reduced (< 2-fold) in the presence of 4-MU. Figure S1-B, C and D show that m-Akt expression attenuated the effect of 4-MU on cell growth, apoptosis and NFkB reporter activity. Expression of myr-Akt also reversed the inhibitory effect of 4-MU on IL-8, HAS2, RHAMM, CD44 and MMP-9 expression (Figure S1-E). However, myr-Akt expression did not alter the 4-MU induced down regulation of Caveolin-1, CXCR1, CXCR7, and CXCR4 mRNAs (data not shown).

Effect of 4-MU on tumor growth and angiogenesis

Effect of 4-MU treatment by oral gavage on PC3-ML xenografts is shown in Figure 6 A. 4-MU significantly inhibited tumor growth at both, 225 mg/kg and 450 mg/kg, doses ($P < 0.001$; Bonferroni's multiple comparison test). Tumor weight at necropsy in the vehicle treated group (299.4 ± 81.5) was three times higher than in the 4-MU treated groups (225 mg/kg: 112.9 ± 21.9; 83 ± 16.1). Unlike coumerin which causes loss of body weight and reduction in prostate, testis and seminal vesicle weights (43), the 4-MU treatment (450 mg/kg) did not cause such reductions ($P > 0.05$ Figure S2- A and B; supplement). 4-MU also did not cause gross histological changes in prostate, testis, seminal vesicles, liver, kidney and lung tissues (data not shown). Serum chemistry analysis showed no significant differences in blood urea nitrogen, creatinine, SGPT, and alkaline phosphatase levels from vehicle and 4-MU treated (450 mg/kg) animals ($P > 0.05$; Table 3, supplement); blood clotting time is also similar in both groups.

We next determined whether 4-MU delayed tumor growth if the treatment started after the tumors become palpable (7^{th} day). As shown in Figure 6 B, 4-MU (450 mg/kg) significantly slowed tumor growth ($P < 0.001$ at each time point). Tumor weight at necropsy in the vehicle treated group (338 ± 131) was 4-fold higher than in 4-MU treated groups (79 ± 37.2; $P < 0.001$).

Analyses of tumor tissue extracts from the experiment described in Figure 6 A showed increased levels of activated caspase-8, caspase-9, caspase-3, cleaved PARP and DR4 and decreased levels of CD44, RHAMM, HAS2 and caveolin-1 in tumor extracts from 4-MU treated animals. This suggests that 4-MU reduces tumor growth by increasing apoptosis and decreasing the expression of HA receptors and related molecules.

Figure 6 D shows decreased HA production in tumor-associated stroma and tumor cells in the specimen from 4-MU treated animals when compared to vehicle treated animals. As shown in Figure 6 D, a tumor specimen from the 4-MU treated group had lower MVD than the vehicle treated tumor. MVD (mean ± sd) in tumors from 4-MU-treated animals was 3.3-fold lower (10.8 ± 4.3) than in the vehicle treated animals (33.4 ± 9.1; $P < 0.001$). Since MVD was calculated as the number of microvessels per high power field, the observed decrease in MVD was most likely independent of tumor size or volume. On the contrary, an increase in TUNEL positive cells was observed in tumor specimens from 4-MU treated animals, when compared to vehicle treated animals (Figure 6 D). The apoptosis index in tumor specimens from the 4-MU treated group was 5-times higher (61.4 ±17.1) when compared to the vehicle group (12.8 ± 7.7; $P < 0.001$).

Taxotere® (TXTR) is approved for the treatment of castration resistant prostate cancer. In PC3-ML xenograft models, 20 mg/kg weekly dose of TXTR has been shown to cause 62% inhibition of tumor growth (44). Therefore, we examined whether the combination of 4-MU and TXTR might be more effective in inhibiting PC3-ML cell proliferation than individual treatments alone. As shown in Figure S4-supplement, 4-MU enhanced the cytotoxicity of docetaxel at each dose. At each 4-MU concentration with fixed TXTR concentration or at TXTR concentration with fixed 4-MU concentration, the growth inhibition caused by the combination was higher than each individual drug ($P < 0.01$ to $P < 0.0001$; Bonferroni multiple comparison test).

DISCUSSION

In this study we demonstrate that 4-MU, a dietary supplement and a HA synthesis inhibitor, is a potent apoptotic agent with strong anti-invasive and anti-angiogenic properties against prostate cancer cells. Since 4-MU inhibits HA synthesis primarily by depleting UGA and the Km of UGA-transferase and HA-synthases is 100 – 200 μM (35–37), the IC_{50} of 4-MU for inhibition of HA synthesis is in high micromolar range. 4-MU is a small molecular weight compound (198 Dalton) and has been used as a choleretic agent in clinical trials for Hepatitis B and C at 2.2 g/day dose (Clinicaltrials.gov Identifer: NCT00225537). Therefore, administration of 4-MU at high micromolecular concentrations is feasible.

4-MU is a strong inducer of apoptosis in prostate cancer cells. Furthermore, the IC_{50} for HA synthesis inhibition and induction of apoptosis (0.4 mM) are the same in all five prostate cancer cell lines, regardless of their androgen sensitivity. Since addition of HA preventes inhibitory effects of 4-MU on cell proliferation and apoptosis, it indicates that 4-MU induces such effects by inhibiting HA synthesis. Up-regulation of Fas-L, Fas, DR4 and FADD by 4-MU suggests that apoptosis induction by 4-MU involves the death receptor pathway. We have previously reported that HAS1 knockdown increases Fas and FADD expression, and transcriptionally down regulates CD44 (16). CD44 has been shown to regulate death-receptor mediated apoptosis (45). However, 4-MU also induces apoptosis in cell lines which do not express CD44 (e.g., LNCaP and LAPC-4; ref 46). All prostate cancer cell lines used in this study express RHAMM (unpublished results). RHAMM-HA interaction also induces PI3-kinase signaling, which in turn, promote survival by down regulating Fas and death receptor signaling (47). The data in Figure 3 D and 4B show that addition of HA prevented the 4-MU induced down-regulation of CD44 and RHAMM both at protein and mRNA levels. The availability of HA receptors may explain why addition of HA is able to prevent the 4-MU induced apoptosis and motility in a significant manner.

PI3-kinase/Akt signaling is known to promote survival by down regulating Fas and death receptor signaling (48). Since myr-Akt expression prevents effect of 4-MU on cell growth, apoptosis and gene expression, it indicates that inhibition of Akt signaling is an important mechanism in the antitumor activity of 4-MU. NFkB activation induces the expression of chemokines and chemokine receptors (25–30). Akt signaling regulates CXCR4, which may regulate CXCR7, and CD44 may be a downstream target of CXCR7 (49). Since HA either completely or partially prevents the 4-MU induced decrease in CXCR1, CXCR4, CXCR-7 and IL-8 expression, the inhibitory effect of 4-MU on the expression of these genes is likely through the inhibition of HA synthesis. 4-MU is a strong inhibitor of caveolin-1 expression; however, this inhibition is independent of the inhibitory effect of 4-MU on HA synthesis and subsequent Akt activation.

Our data show that 4-MU inhibits tumor growth in the PC3-ML xenograft model. Since HA increases hydration and opens up spaces in tissues, it is possible that the observed decrease in tumor volumes in 4-MU-treated animals is not due to decreased tumor burden. However, the

tumor weight in 4-MU treated animals was 4-times lower than in the vehicle treated animals. HA is present in tumor tissues in microgram amounts (50), and therefore, the decrease in HA amount (and consequently, decreased water content) due to 4-MU treatment cannot possibly account for the decrease in tumor weight which is in milligrams. Furthermore, the increased apoptosis index in 4-MU treated tumors supports the notion that the decrease in tumor volume/weight observed in 4-MU treated tumors is due to smaller tumor burden.

The trend observed in cell culture studies regarding down regulation of CD44, RHAMM, HAS2 and caveolin-1 and up regulation of apoptosis signaling proteins is also present in 4-MU treated tumor tissues. The decrease in RHAMM and CD44 in 4-MU treated tumor tissues (≥ 50%; Figure 6) is less than the decrease observed in cell culture studies (≥ 80%). The differences observed in tumor specimens and cell culture experiments may be due to the fact that the observed CD44 and RHAMM levels in tumor tissue extracts are contributed by both tumor cells and stromal components. The effect of 4-MU on the latter is currently unknown.

Our study shows that 4-MU is a potent, orally bioavailable and relatively non-toxic anti-cancer agent with significant anti-invasive, anti-angiogenic and possibly anti-inflammatory properties. Since 4-MU down regulates HA receptors, HAS2 and caveolin-1 expression and Akt signaling, it may be a better therapeutic approach than targeting individual HA receptors.

Supplementary Material

Refer to Web version on PubMed Central for supplementary material.

Acknowledgments

Grant support: R01 CA 123063-03 (VBL); R01CA72821-09 (VBL)

We dedicate this article to the memory of our colleague Ms. Neetika Dhir. We thank Mrs. Cynthia Soloway for critically reviewing this manuscript.

Abbreviations used

HA	hyaluronic acid
HAS	hyaluronic acid synthase
4-MU	4-methylumbelliferone
SDF-1	stromal cell-derived factor-1
UGA	UDP-glucuronic acid

REFERENCES

1. Volpi N, Schiller J, Stern R, Soltés L. Role, metabolism, chemical modifications and applications of hyaluronan. Curr Med Chem 2009;16:1718–1745. [PubMed: 19442142]
2. Ekici S, Cerwinka WH, Duncan R, et al. Comparison of the prognostic potential of hyaluronic acid, hyaluronidase (HYAL-1), CD44v6 and microvessel density for prostate cancer. Int J Cancer 2004;112:121–129. [PubMed: 15305383]
3. Posey JT, Soloway MS, Ekici S, et al. Evaluation of the prognostic potential of hyaluronic acid and hyaluronidase (HYAL1) for prostate cancer. Cancer Res 2003;63:2638–2644. [PubMed: 12750291]
4. Aaltomaa S, Lipponen P, Tammi R, et al. Strong Stromal Hyaluronan Expression Is Associated with PSA Recurrence in Local Prostate Cancer. Urol Int 2002;69:266–272. [PubMed: 12444281]
5. Gomez C, Gomez P, Knapp J, et al. Hyaluronic acid and HYAL-1 expression in prostate biopsy specimens: Predictors of biochemical recurrence. J Urol. 2009 (In Press).

6. Lokeshwar VB, Rubinowicz D, Schroeder GL, et al. Stromal and epithelial expression of tumor markers hyaluronic acid and HYAL1 hyaluronidase in prostate cancer. J Biol Chem 2001;276:11922–11932. [PubMed: 11278412]
7. Simpson MA, Lokeshwar VB. Hyaluronan and hyaluronidase in genitourinary tumors. Front Biosci 2008;13:5664–5680. [PubMed: 18508614]
8. Itano N, Atsumi F, Sawai T, et al. Abnormal accumulation of hyaluronan matrix diminishes contact inhibition of cell growth and promotes cell migration. Proc Natl Acad Sci U S A 2002;99:3609–3614. [PubMed: 11891291]
9. Kerbel RS, St Croix B, Florenes VA, Rak J. Induction and reversal of cell adhesion-dependent multicellular drug resistance in solid breast tumors. Hum Cell 1996;9:257–264. [PubMed: 9183656]
10. Itano N, Sawai T, Yoshida M, et al. Three isoforms of mammalian hyaluronan synthases have distinct enzymatic properties. J Biol Chem 1999;274:25085–25092. [PubMed: 10455188]
11. Itano N, Sawai T, Atsumi F, et al. Selective expression and functional characteristics of three mammalian hyaluronan synthases in oncogenic malignant transformation. J Biol Chem 2004;279:18679–18687. [PubMed: 14724275]
12. Itano N, Kimata K. Altered hyaluronan biosynthesis in cancer progression. Semin Cancer Biol 2008;18:268–274. [PubMed: 18450474]
13. Bharadwaj AG, Kovar JL, Loughman E, Elowsky C, Oakley GG, Simpson MA. Spontaneous metastasis of prostate cancer is promoted by excess hyaluronan synthesis and processing. Am J Pathol 2009;174:1027–1036. [PubMed: 19218337]
14. Bharadwaj AG, Rector K, Simpson MA. Inducible hyaluronan production reveals differential effects on prostate tumor cell growth and tumor angiogenesis. J Biol Chem 2007;282:20561–20572. [PubMed: 17502371]
15. Simpson MA, Wilson CM, McCarthy JB. Inhibition of prostate tumor cell hyaluronan synthesis impairs subcutaneous growth and vascularization in Immunocompromised mice. Am J Pathol 2002;161:849–857. [PubMed: 12213713]
16. Golshani R, Lopez L, Estrella V, Kramer M, Iida N, Lokeshwar VB. Hyaluronic acid synthase-1 expression regulates bladder cancer growth, invasion, and angiogenesis through CD44. Cancer Res 2008;68:483–491. [PubMed: 18199543]
17. Li Y, Li L, Brown TJ, Heldin P. Silencing of hyaluronan synthase 2 suppresses the malignant phenotype of invasive breast cancer cells. Int J Cancer 2007;120:2557–2567. [PubMed: 17315194]
18. Lokeshwar VB, Cerwinka WH, Isoyama T, Lokeshwar BL. HYAL1 hyaluronidase in prostate cancer: a tumor promoter and suppressor. Cancer Res 2005;65:7782–7789. [PubMed: 16140946]
19. Lokeshwar VB, Cerwinka WH, Lokeshwar BL. HYAL1 hyaluronidase: a Molecular determinant of bladder tumor growth and invasion. Cancer Res 2005;65:2243–2250. [PubMed: 15781637]
20. Misra S, Toole BP, Ghatak S. Hyaluronan constitutively regulates activation of multiple receptor tyrosine kinases in epithelial and carcinoma cells. J Biol Chem 2006;281:34936–34941. [PubMed: 16959784]
21. Ghatak S, Misra S, Toole BP. Hyaluronan constitutively regulates ErbB2 phosphorylation and signaling complex formation in carcinoma cells. J Biol Chem 2005;280:8875–8883. [PubMed: 15632176]
22. Bourguignon LY, Spevak CC, Wong G, Xia W, Gilad E. Hyaluronan-CD44 Interaction with PKC-epsilon promotes oncogenic signaling by the stem cell marker, Nanog and the production of microRNA-21 leading to downregulation of the tumor suppressor protein, PDCD4, anti-apoptosis and chemotherapy resistance in breast tumor cells. J Biol Chem. 2009 [Epub ahead of print].
23. Kim Y, Lee YS, Choe J, Lee H, Kim YM, Jeoung D. CD44-epidermal growth factor receptor interaction mediates hyaluronic acid-promoted cell motility by activating protein kinase C signaling involving Akt, Rac1, Phox, reactive oxygen species, focal adhesion kinase, and MMP-2. J Biol Chem 2008;283:22513–22528. [PubMed: 18577517]
24. Murray D, Morrin M, McDonnell S. Increased invasion and expression of MMP-9 in human colorectal cell lines by a CD44-dependent mechanism. Anticancer Res 2004;24:489–494. [PubMed: 15152948]
25. Desai B, Rogers MJ, Chellaiah MA. Mechanisms of osteopontin and CD44 as metastatic principles in prostate cancer cells. Mol Cancer 2007;6:18. [PubMed: 17343740]

26. Horton MR, Boodoo S, Powell JD. NF-kappa B activation mediates the cross-talk between extracellular matrix and interferon-gamma (IFN-gamma) leading to enhanced monokine induced by IFN-gamma (MIG) expression in macrophages. J Biol Chem 2002;277:43757–43762. [PubMed: 12226082]
27. Voelcker V, Gebhardt C, Averbeck M, et al. Hyaluronan fragments induce cytokine and metalloprotease upregulation in human melanoma cells in part by signalling via TLR4. Exp Dermatol 2008;17:100–107. [PubMed: 18031543]
28. Mascarenhas MM, Day RM, Ochoa CD, et al. Low molecular weight hyaluronan from stretched lung enhances interleukin-8 expression. Am J Respir Cell Mol Biol 2004;30:51–60. [PubMed: 12738686]
28. Haslinger B, Mandl-Weber S, Sellmayer A, Sitter T. Hyaluronan fragments induce the synthesis of MCP-1 and IL-8 in cultured human peritoneal mesothelial cells. Cell Tissue Res 2001;305:79–86. [PubMed: 11512674]
29. Tonnarelli B, Manferdini C, Piacentini A, et al. Surface-dependent modulation of proliferation, bone matrix molecules, and inflammatory factors in human osteoblasts. J Biomed Mater Res A 2009;89:687–696. [PubMed: 18442123]
30. Lisignoli G, Cristino S, Piacentini A, Cavallo C, Caplan AI, Facchini A. Hyaluronan-based polymer scaffold modulates the expression of inflammatory and degradative factors in mesenchymal stem cells: Involvement of Cd44 and Cd54. J Cell Physiol 2006;207:364–373. [PubMed: 16331675]
31. Araki S, Omori Y, Lyn D, et al. Interleukin-8 is a molecular determinant of androgen independence and progression in prostate cancer. Cancer Res 2007;67:6854–6862. [PubMed: 17638896]
32. Rilla K, Pasonen-Seppanen S, Rieppo J, Tammi M, Tammi R. The hyaluronan synthesis inhibitor 4-methylumbelliferone prevents keratinocyte activation and epidermal hyperproliferation induced by epidermal growth factor. J Invest Dermatol 2004;123:708–714. [PubMed: 15373776]
33. Kudo D, Kon A, Yoshihara S, Kakizaki I, Sasaki M, Endo M, Takagaki K. Effect of a hyaluronan synthase suppressor, 4-methylumbelliferone, on B16F-10 melanoma cell adhesion and locomotion. Biochem Biophys Res Commun 2004;321:783–787. [PubMed: 15358095]
34. Yoshihara S, Kon A, Kudo D, et al. A hyaluronan synthase suppressor, 4-methylumbelliferone, inhibits liver metastasis of melanoma cells. FEBS Lett 2005;579:2722–2726. [PubMed: 15862315]
35. Kakizaki I, Kojima K, Takagaki K, et al. A novel mechanism for the inhibition of hyaluronan biosynthesis by 4-methylumbelliferone. J Biol Chem 2004;279:33281–33289. [PubMed: 15190064]
36. Kakizaki I, Takagaki K, Endo Y, et al. Inhibition of hyaluronan synthesis in Streptococcus equi FM100 by 4-methylumbelliferone. Eur J Biochem 2002;269:5066–5075. [PubMed: 12383266]
37. Morohashi H, Kon A, Nakai M, et al. Study of hyaluronan synthase inhibitor, 4-methylumbelliferone derivatives on human pancreatic cancer cell (KP1-NL). Biochem Biophys Res Commun 2006;345:1454–1459. [PubMed: 16730656]
38. Kultti A, Pasonen-Seppänen S, Jauhiainen M, et al. 4-Methylumbelliferone inhibits hyaluronan synthesis by depletion of cellular UDP-glucuronic acid and downregulation of hyaluronan synthase 2 and 3. Exp Cell Res 2009;315:1914–1923. [PubMed: 19285976]
39. Lokeshwar VB, Gomez P, Kramer M, et al. Epigenetic regulation of HYAL-1 hyaluronidase expression. identification of HYAL-1 promoter. J Biol Chem 2008;283:29215–29227. [PubMed: 18718911]
40. Lokeshwar VB, Estrella V, Lopez L, et al. HYAL1-v1, an alternatively spliced variant of HYAL1 hyaluronidase: a negative regulator of bladder cancer. Cancer Res 2006;66:11219–11227. [PubMed: 17145867]
41. Lokeshwar BL, Lokeshwar VB, Block NL. Expression of CD44 in prostate cancer cells: association with cell proliferation and invasive potential. Anticancer Res 1995;15:1191–1198. [PubMed: 7544562]
42. Thompson TC, Tahir SA, Li L, et al. The role of caveolin-1 in prostate cancer: clinical implications. Prostate Cancer Prostatic Dis. 2009 Jul 7; [Epub ahead of print].
43. Omarbasha B, Fair WR, Heston WD. Effect of coumarin on the normal rat prostate and on the R-3327H prostatic adenocarcinoma. Cancer Res 1989;49:3045–3049. [PubMed: 2720665]
44. Liu G, Taylor SA, Marrinan CH, Hsieh Y, Bishop WR, Kirschmeier P, Long BJ. Continuous and intermittent dosing of lonafarnib potentiates the therapeutic efficacy of docetaxel on preclinical human prostate cancer models. Int J Cancer 2009;125:2711–2720. [PubMed: 19530253]

45. Hauptschein RS, Sloan KE, Torella C, et al. Functional proteomic screen identifies a modulating role for CD44 in death receptor-mediated apoptosis. Cancer Res 2005;65:1887–1896. [PubMed: 15753387]

46. Freedland SJ, Seligson DB, Liu AY, et al. Loss of CD10 (neutral endopeptidase) is a frequent and early event in human prostate cancer. Prostate 2003;55:71–80. [PubMed: 12640663]

47. Gouëffic Y, Guilluy C, Guérin P, Patra P, Pacaud P, Loirand G. Hyaluronan induces vascular smooth muscle cell migration through RHAMM-mediated PI3K-dependent Rac activation. Cardiovasc Res 2006;72:339–348. [PubMed: 16934786]

48. Kim MJ, Kim HB, Bae JH, et al. Sensitization of human K562 leukemic cells to TRAIL-induced apoptosis by inhibiting the DNA-PKcs/Akt-mediated cell survival pathway. Biochem Pharmacol 2009;78:573–582. [PubMed: 19464267]

49. Wang J, Shiozawa Y, Wang J, et al. The role of CXCR7/RDC1 as a chemokine receptor for CXCL12/SDF-1 in prostate cancer. J Biol Chem 2008;283:4283–4294. [PubMed: 18057003]

50. Lokeshwar VB, Obek C, Soloway MS, Block NL. Tumor-associated hyaluronic acid: a new sensitive and specific urine marker for bladder cancer. Cancer Res 1997;57:773–777. Erratum in: Cancer Res 1998; 58:3191. [PubMed: 9044859]

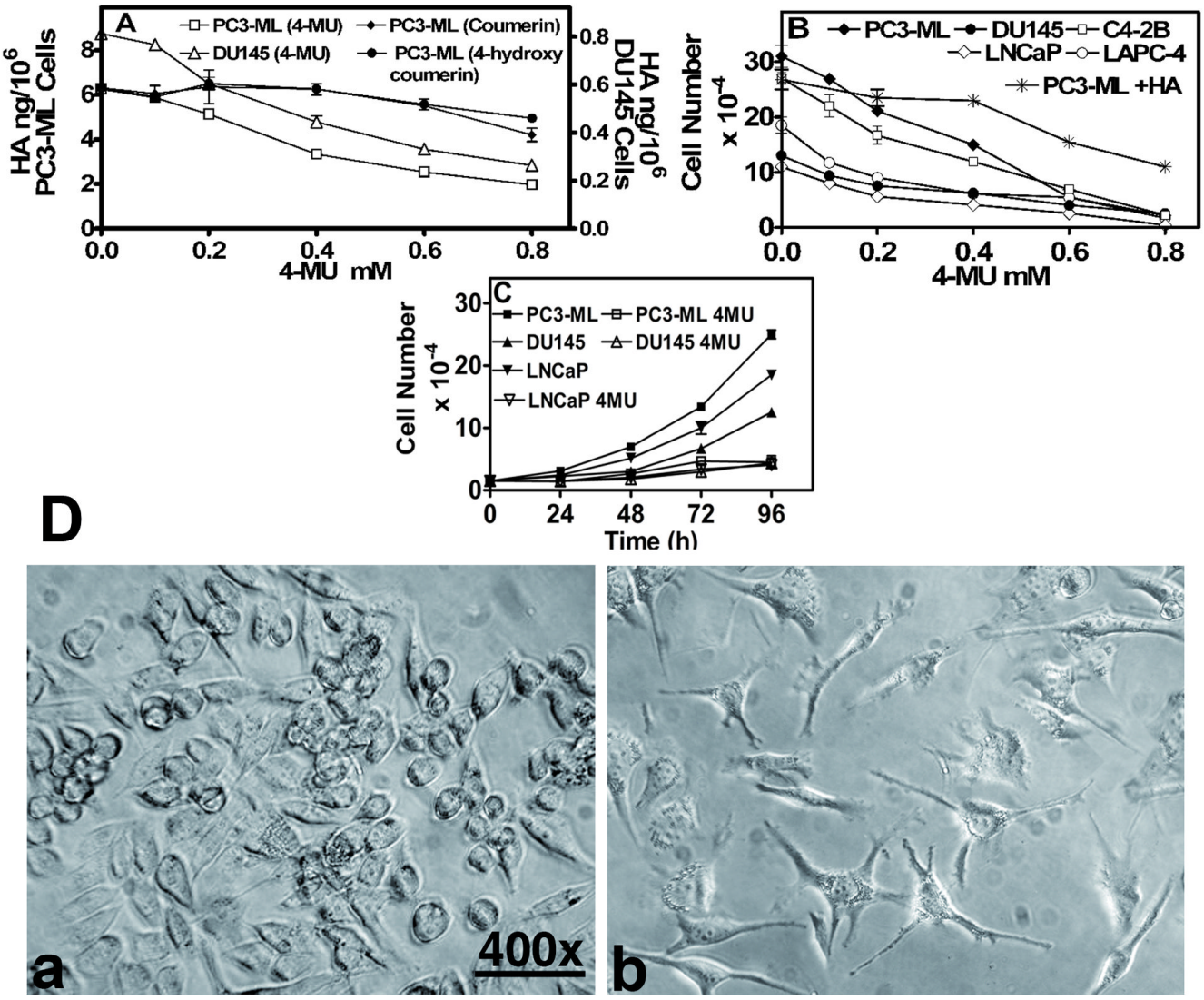

Figure 1. Effect of 4-MU on HA synthesis and cell proliferation

A: Measurement of HA levels by HA ELISA-like assay. Data: Mean ± SEM; 3 experiments. **B and C:** Cell counting data after 72 h treatment with 4-MU (B). In some cases, PC3-ML cells were treated with 4-MU plus 50-μg/ml HA and counted after 72 h (PC3-ML +HA graph). Prostate cancer cells were treated with 4-MU (0.4 mM) and counted every 24 h (C). Data: Mean ± S.D. (triplicate in 2 experiments). **D:** Light microscopy of PC3-ML cells either untreated (a) or treated with 4-MU (0.4 mM; b) for 48 h. Magnification: 400×.

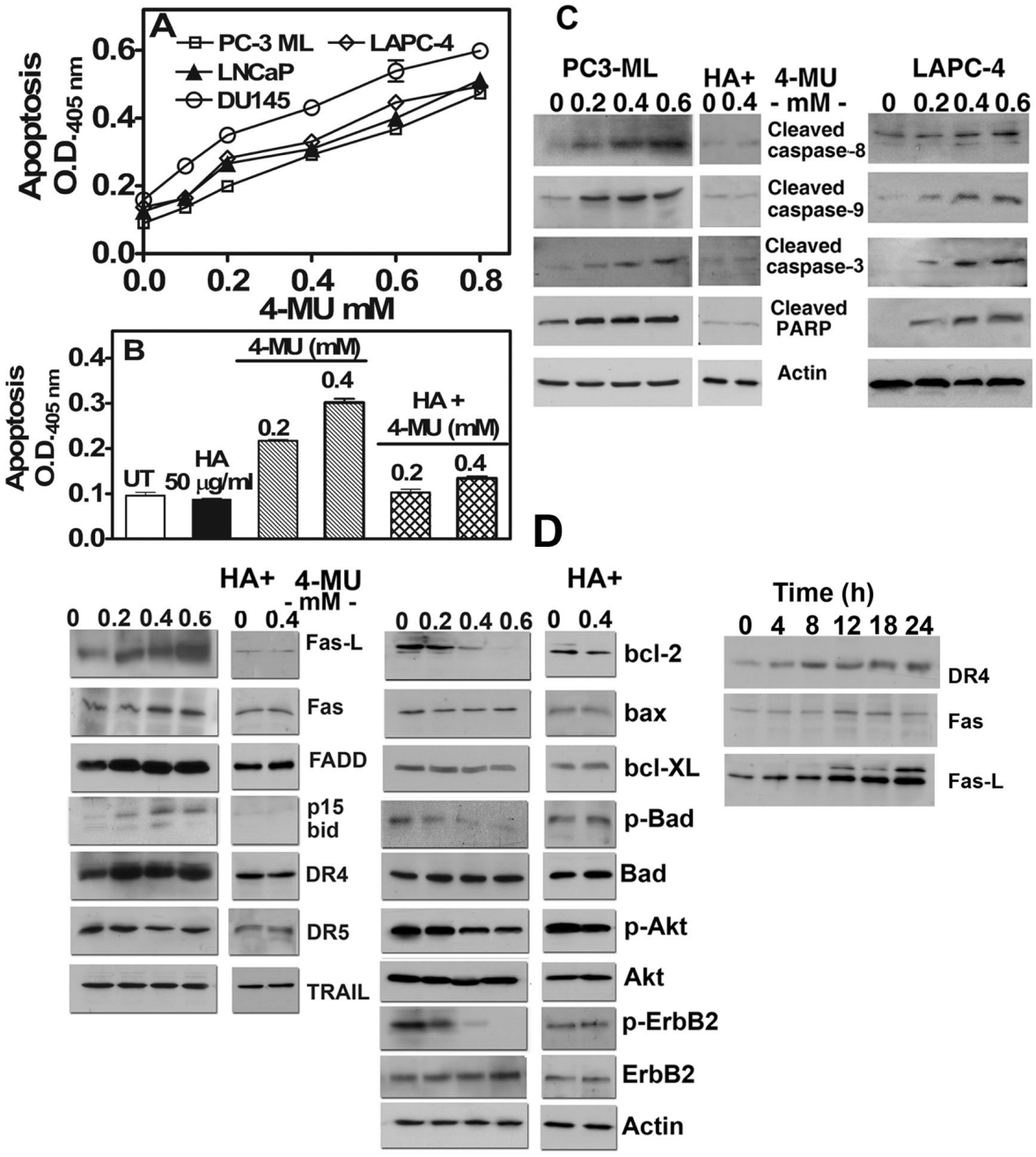

Figure 2. Effect of 4-MU on apoptosis

A: Measurement of apoptosis in cells treated with 4-MU for 48 h. Data: Mean ± S.D. **B:** Measurement of apoptosis in PC3-ML cells treated with 4-MU +/− HA (50-µg/ml) for 48 h. Data: Mean ± S.D. **C and D:** PC3-ML cells treated with 4-MU, were subjected to immunoblot analyses for apoptosis-related proteins. Sub-panel in D: Immunoblot analyses of Fas-L, Fas and DR4 in PC3-ML cells were treated with 4-MU (0.4 mM) for the indicated time periods.

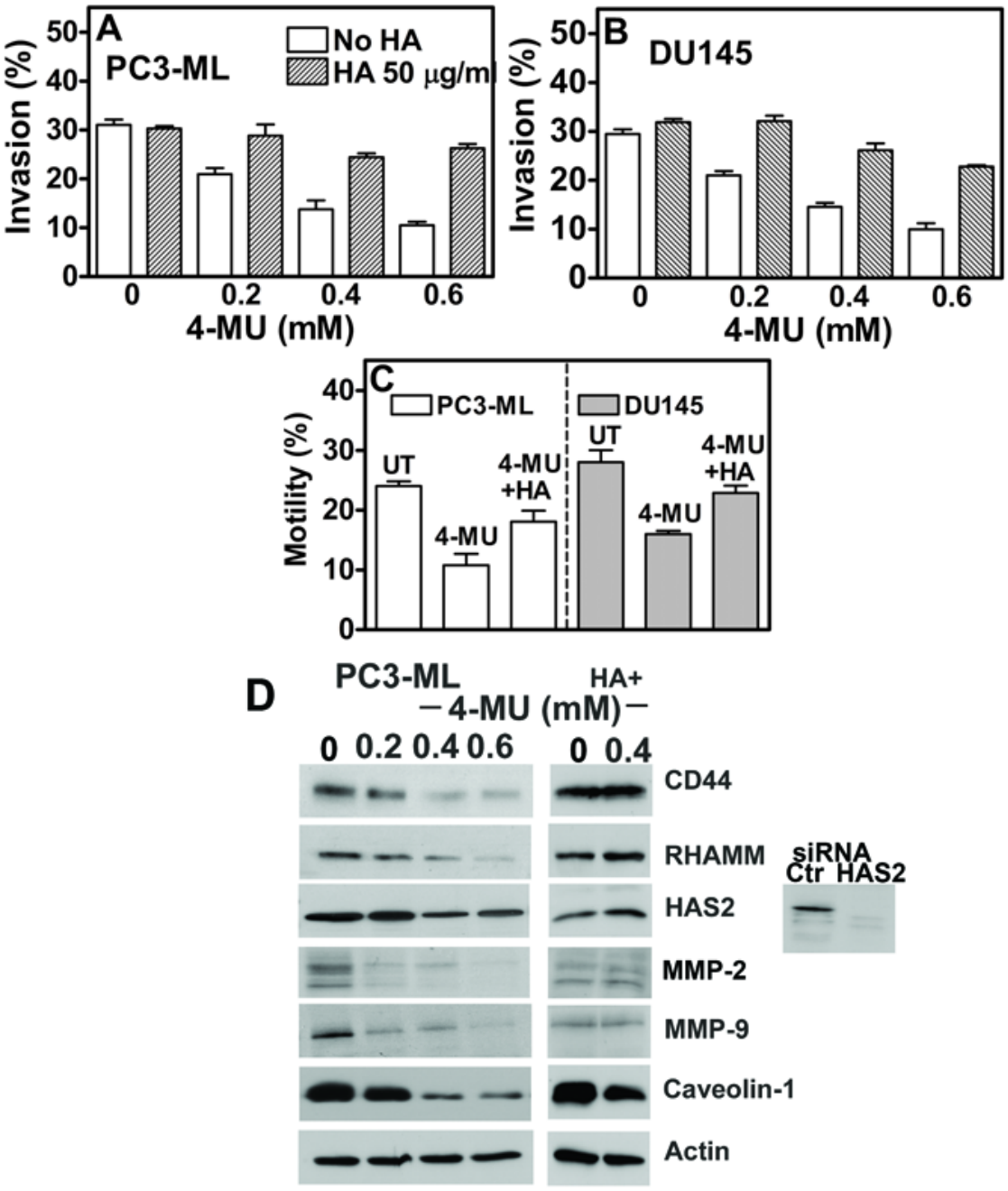

Figure 3. Effect of 4-MU on invasion and chemotactic motility

A and B: Determination of invasive activity of PC3-ML (A) and DU145 (B) cells in the presence or absence of 4-MU and/or HA. Mean ± S.D. (triplicate in 2 experiments). **C.** Determination of chemotactic motility of PC3-ML (A) and DU145 (B) cells in the presence or absence of 4-MU and/or 50-μg/ml HA. Mean ± S.D. **D.** PC3-ML cells treated with 4-MU were subjected to immunoblot analysis. Side panel: PC3-ML cells were transfected with control or HAS2 siRNA and subjected to immunoblot analysis using the anti-HAS2 antibody.

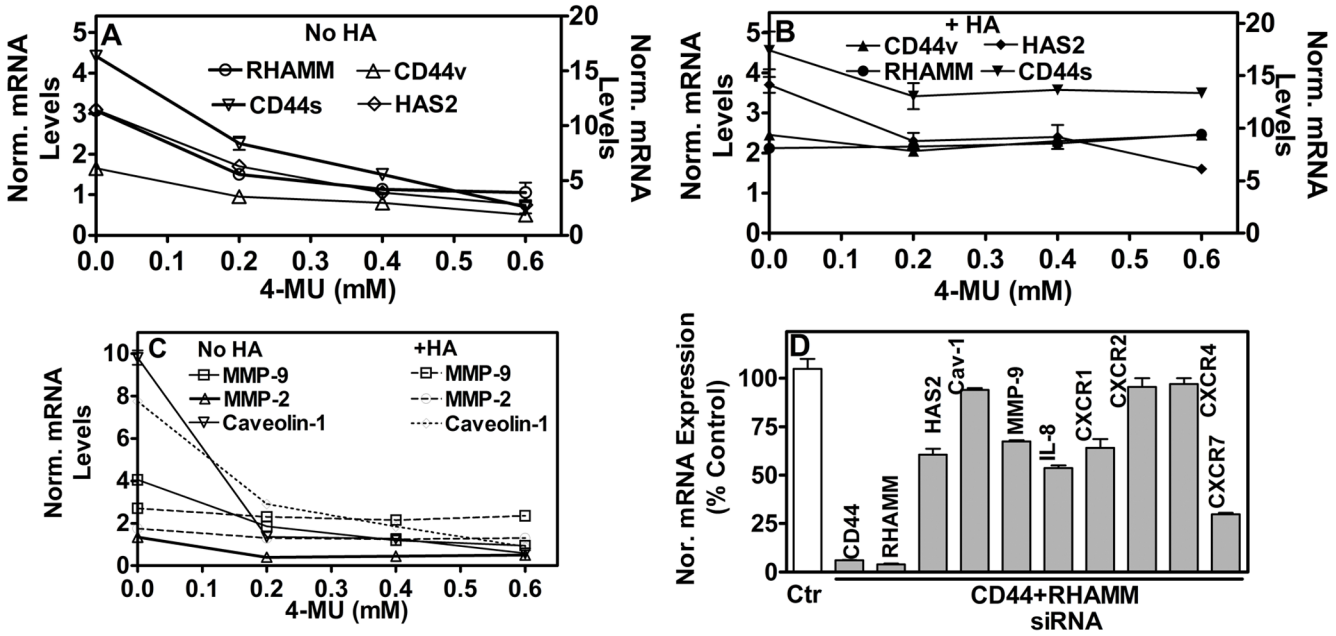

Figure 4. Effect of 4-MU and CD44-RHAMM siRNA-treated cells on gene expression

A, B, C: PC3-ML cells were treated with 4-MU in the absence (A, C) or presence of HA (B, C) and the mRNA levels of indicated genes were assayed by Q-PCR. **D:** PC3-ML cells were treated with CD44 and RHAMM siRNA and the mRNA levels were analyzed by Q-PCR.

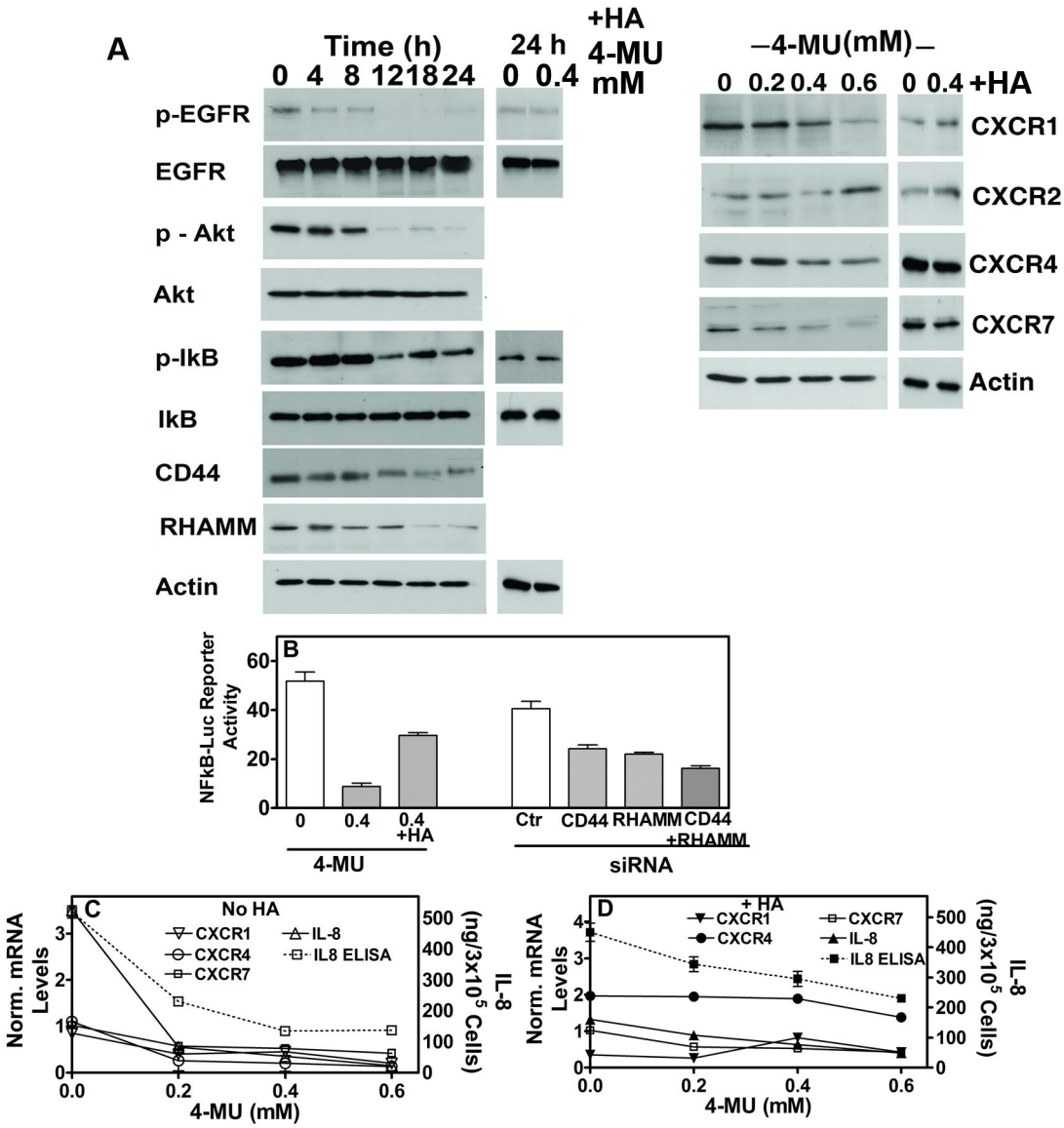

Figure 5. Analysis of HA-related signaling events in 4-MU treated cells

A: Left panel: PC3-ML cells were treated with 0.4 mM 4-MU for various time periods and subjected to immunoblot analyses. Right panel: Immunoblot analyses of CXCR1, CXCR2, CXCR4 and CXCR7 in 4-MU treated PC3-ML cells. **B:** Left panel: PC3-ML cells co-transfected with NFkB promoter Luciferase reporter and Renilla luciferase plasmids were treated with 4-MU (0.4 mM) and/or HA (50 μg/ml). Luciferase activity was measured as described in Materials and Methods. Right panel: NFkB promoter Luciferase reporter activity in PC3-ML cells transfected with control, CD44, RHAMM or CD44 and RHAMM siRNAs. **C and D:** PC3-ML cells were treated with 4-MU in the absence (C) or presence of HA (D). Following 48 h incubation, mRNA levels were determined by Q-PCR.

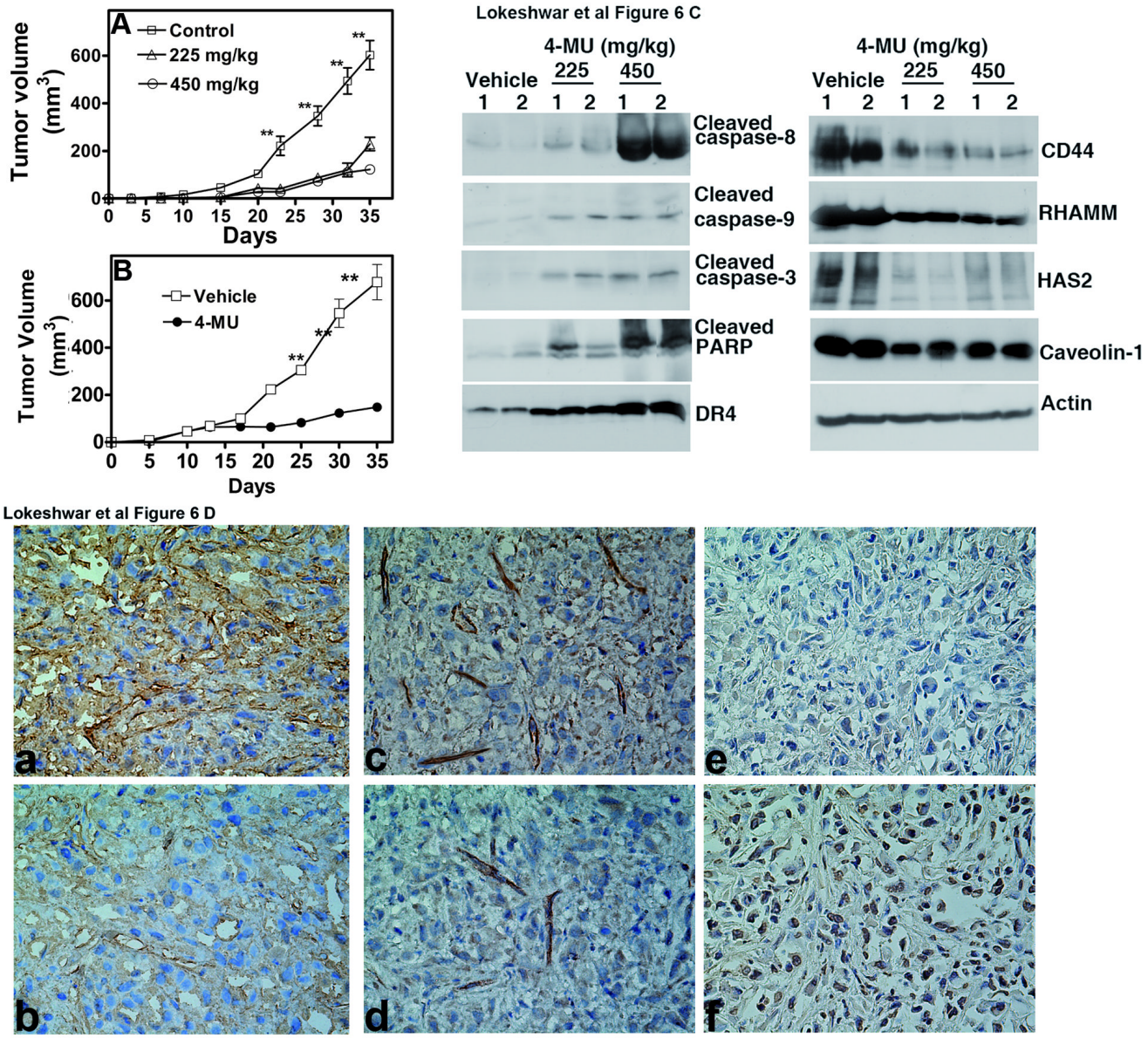

Figure 6. Effect of 4-MU on PC3-ML tumor xenografts

A and B: Athymic mice implanted subcutaneously with PC3-ML cells were orally gavaged twice daily either with vehicle or 4-MU (225 mg/kg or 450 mg/kg). A: Treatment started on the day of the injection. B: Treatment (4-MU: 450 mg/kg) started 7 days post tumor implantation. **C:** Immunoblot analyses of tumor tissue extracts from vehicle and 4-MU treated animals. **D:** HA localization and microvessel density determination by immunohistochemistry: For all panels magnification is 400×. Panels a, b: HA staining; panels c, d: Localization of microvessels. The area of the highest MVD from each specimen is presented here. Panels e, f: TUNEL assay. Panels a, c, e: vehicle; panels b, d, f: 4-MU treatment.